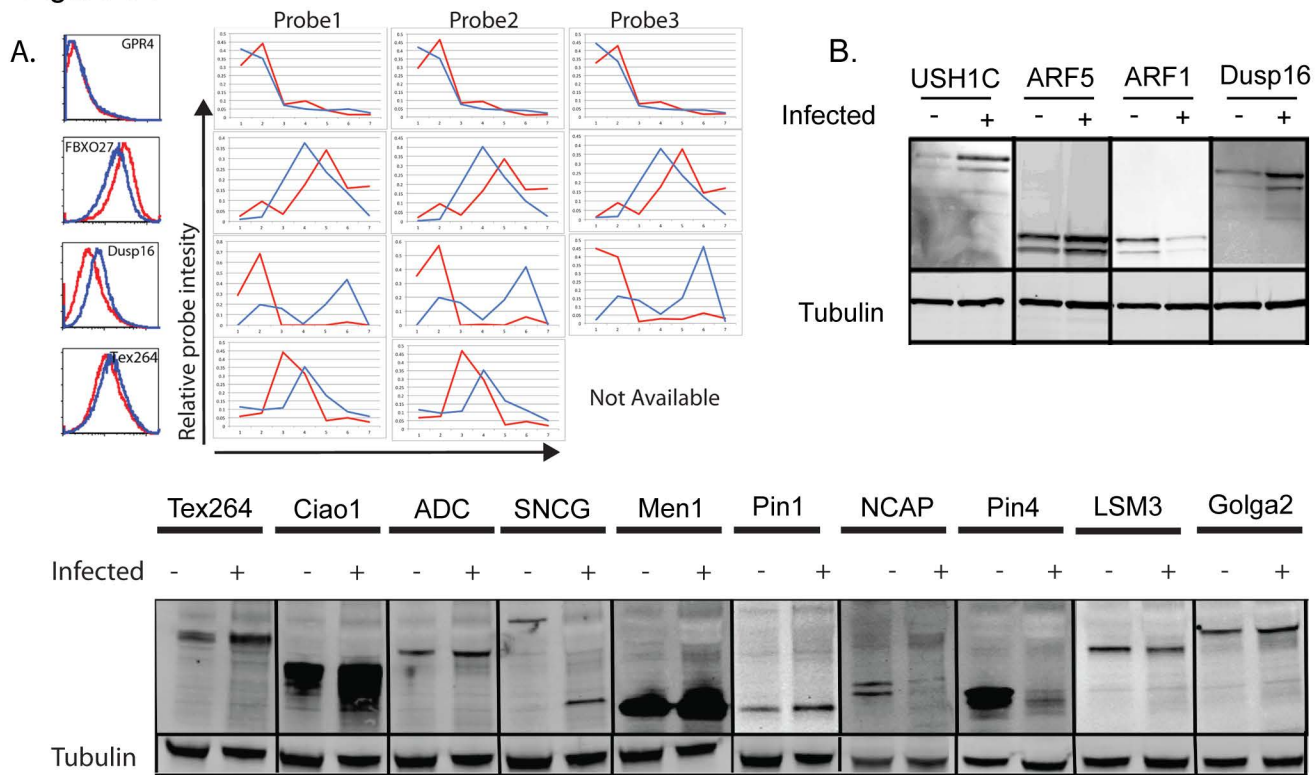


Figure S1



C.

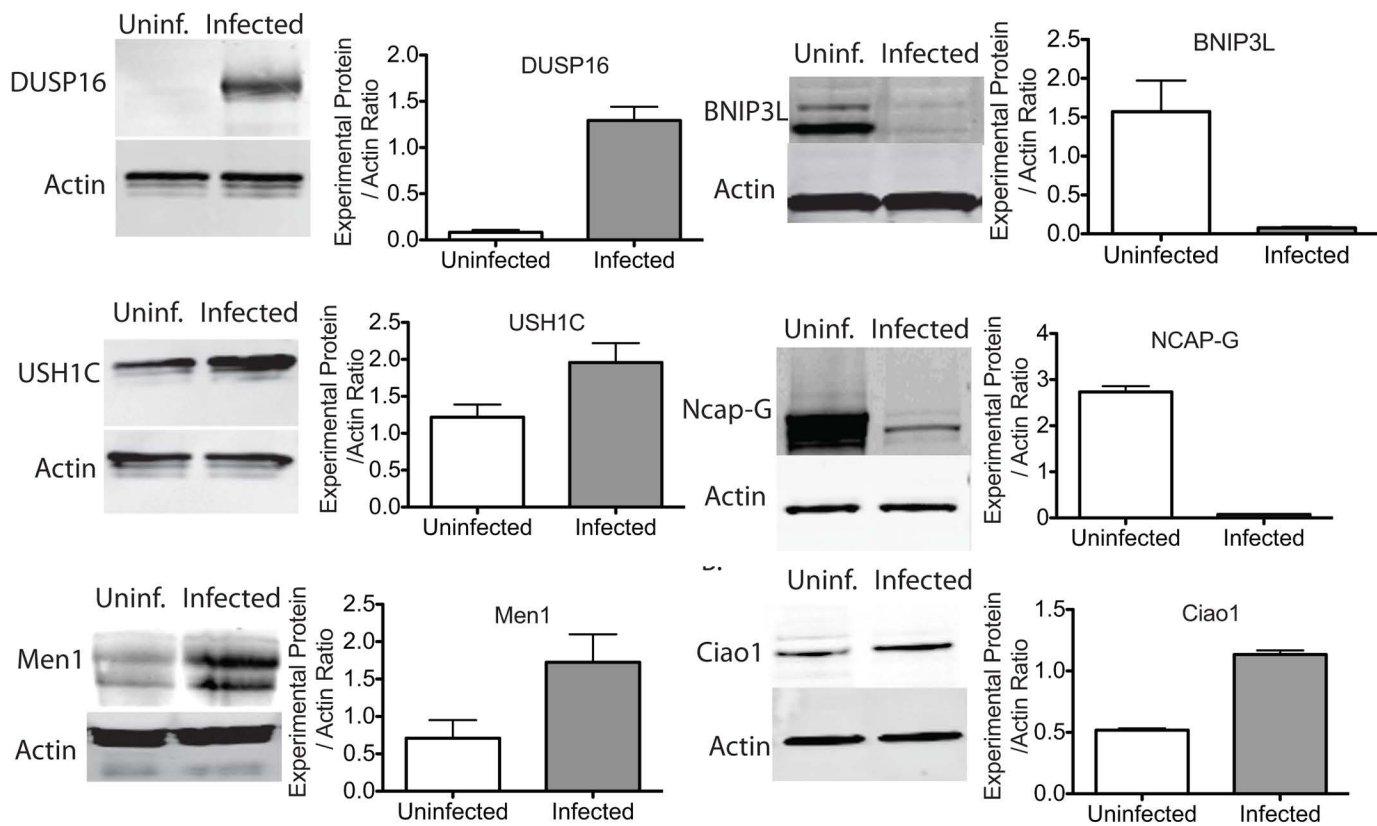
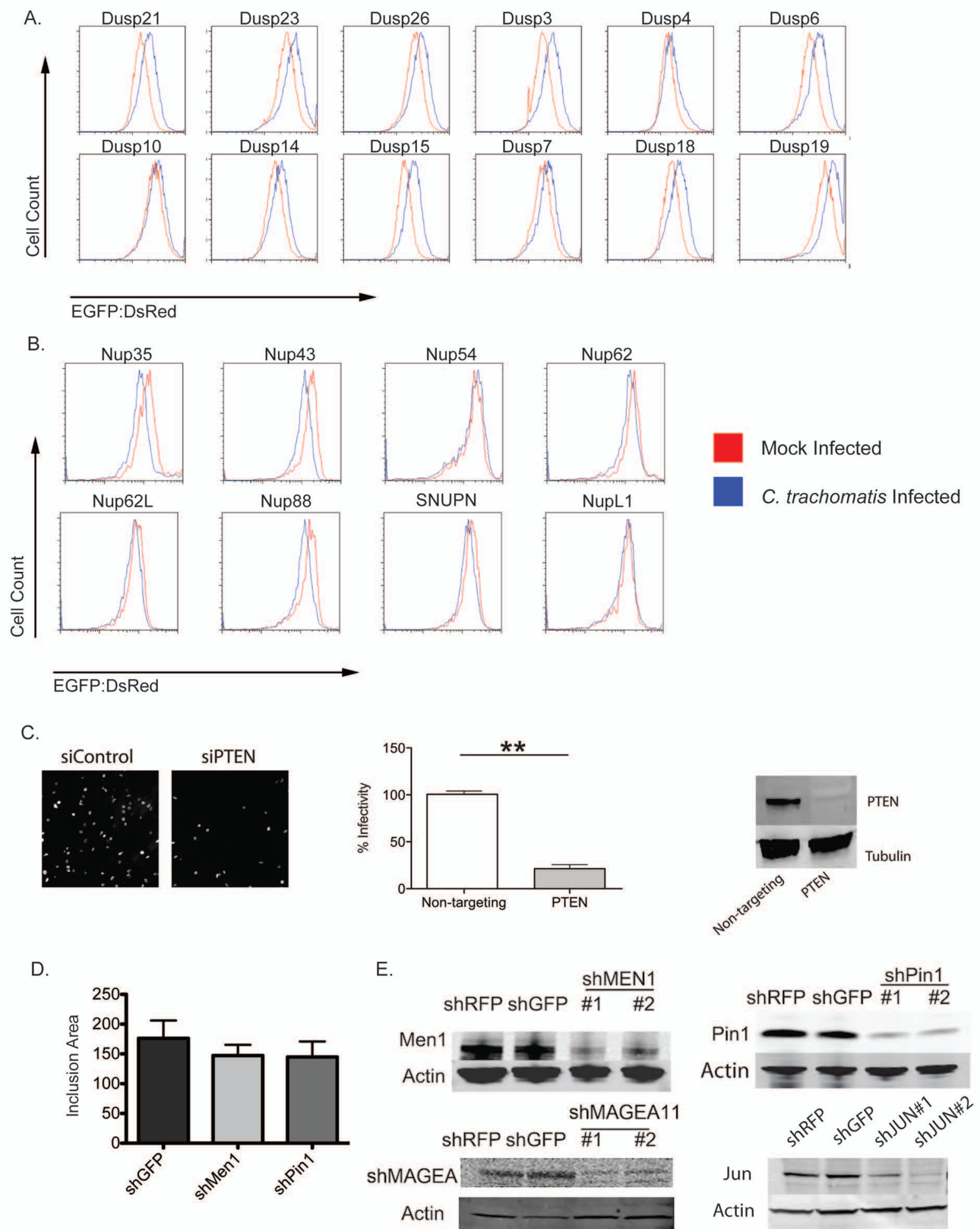
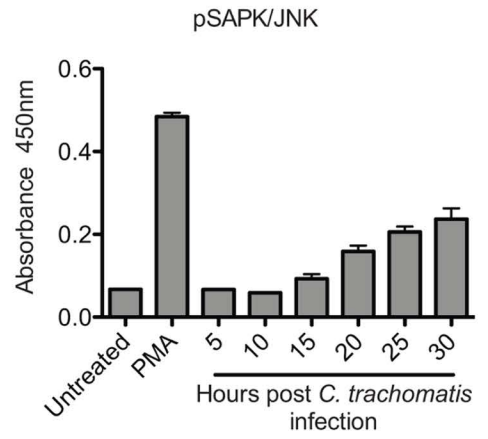
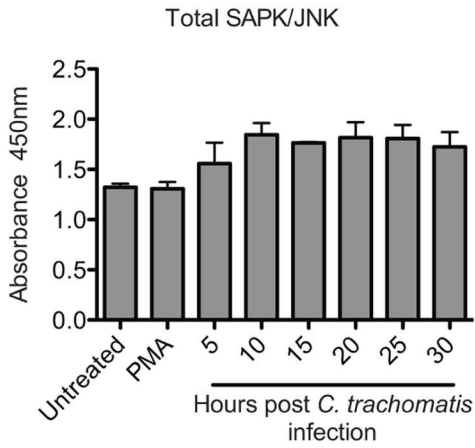


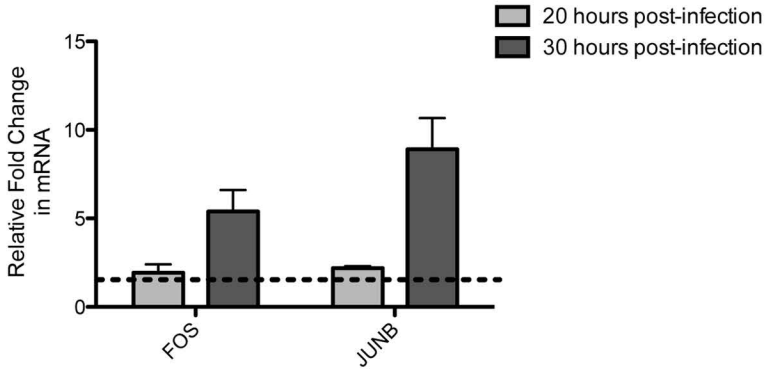
Figure S2



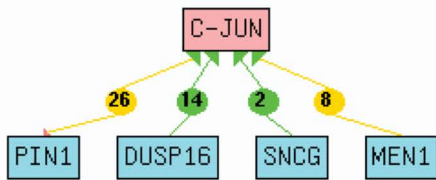
A.



B.



C.



D.

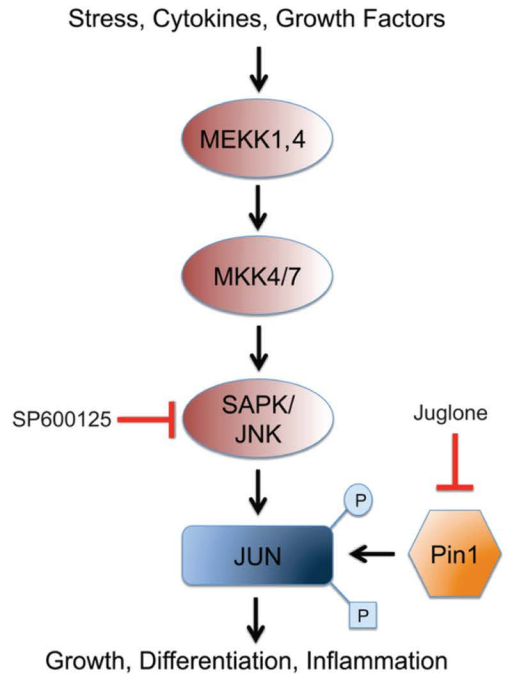
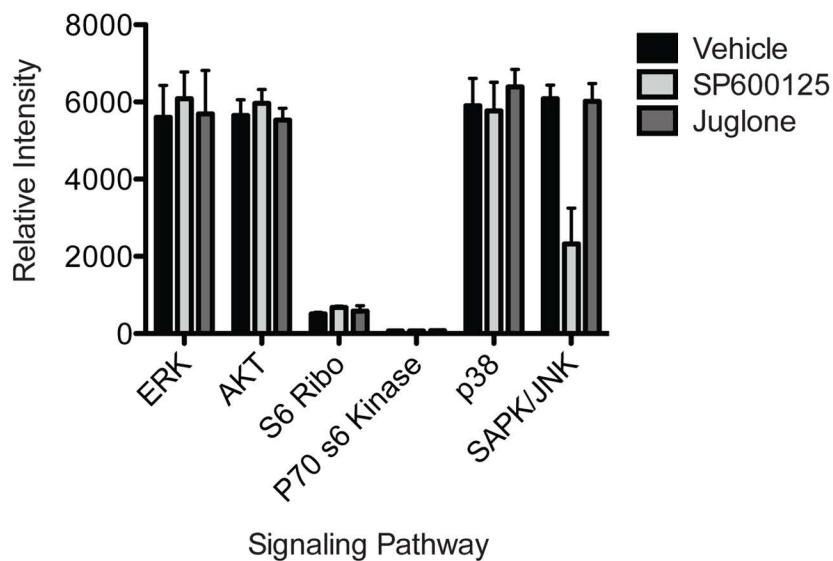


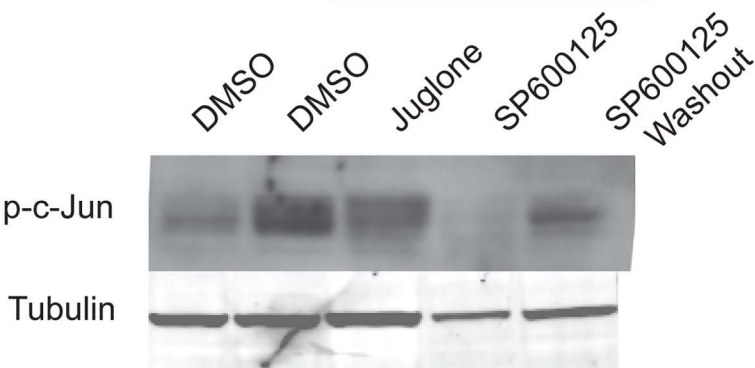
Figure S4

A.

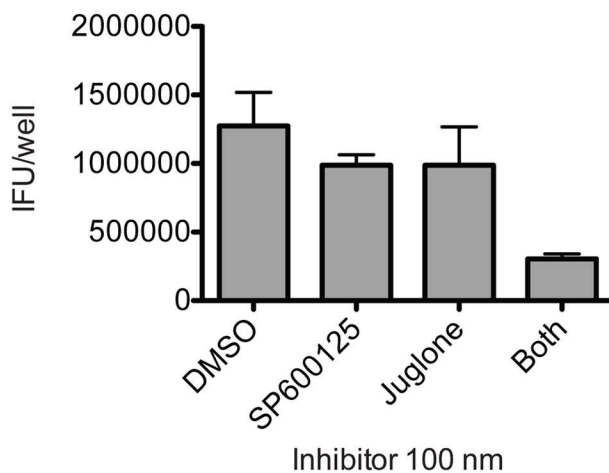


B.

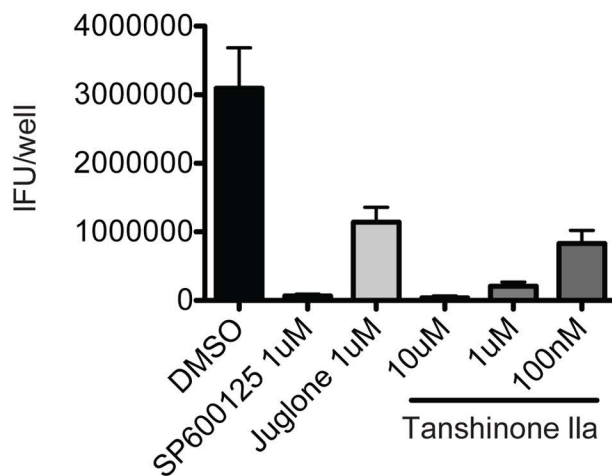
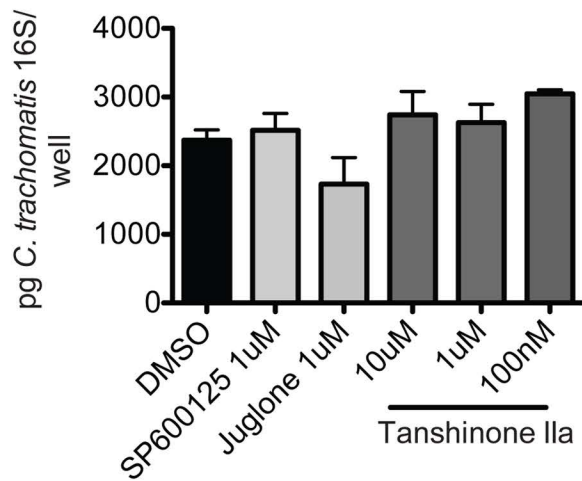
Chlamydia Infection



C.



D.



Supplementary Figure Legends

Figure S1.

A) Infected 293T cells expressing the indicated ORFs in the GPS vector were analyzed by flow cytometry after 24 hours. The microarray probe distributions are shown at the right for probes of the indicated ORFs. A complete list of the validation status of tested proteins can be found in Table S2.

B) A subset of HEK293T cells expressing tagged versions of potential GPS targets were mock-infected or infected with *C. trachomatis* for 24 hours. Cell lysates were analyzed by immunoblot for the indicated experimental proteins and beta tubulin (loading control). Shown are representative blots from one of two independent experiments.

C) 293T cells were mock-infected or infected with *C. trachomatis* for the 30 hours when cells were lysed in 8M Urea. Shown are representative immunoblots for selected proteins (Ciao1, USH1C, DUSP16, Men1, NCAP-G and BNIP3L) and beta-actin (loading control). Replicate samples were quantified using the Odyssey infrared imaging system or imageJ and the relative intensities were plotted in the graphs. Shown are representative blots from one of 3 independent experiments. Related to Figure 1

Figure S2.

A) The entire Dusp family was selected from the ORFeome library and cloned into the GPS vector. 293T cells expressing the indicated ORFs from the Dusp family were made by lentiviral transduction and were analyzed by flow cytometry after 24 hours following infection. Shown are representative plots from one of three independent experiments.

B) The entire Nup family was selected from the ORFeome library and cloned into the GPS vector. 293T cells expressing the indicated ORFs from the Nup family were made using the GPS vector and were analyzed by flow cytometry 24 hours following infection. Shown are representative plots from one of three independent experiments. Related to

Figure 1.

C) Optimization of a loss-of-function screen to identify host factors important for Chlamydia infection. HeLa cells were treated with non-targeting siRNA or siPTEN. Graphs show the mean infectivity relative to the non-targeting siRNA +/- the standard deviation (** $p < .01$)($n=3$). Immunoblot analysis of PTEN and tubulin (loading control) after 72 hour treatment with non-targeting siRNA or siPTEN.

D) Inclusion formation is not disrupted in shRNA knockdown cells. The indicated shRNA cells lines or controls were seeded onto glass coverslips then infected with *C. trachomatis* for 30 hours. Cells were then fixed and stained for the inclusions and host nuclei.

Cells were analyzed by fluorescence microscopy and the mean size of the inclusions was calculated using image J analysis. Shown is a representative experiment of two performed with at least 20 fields per cell line enumerated. $p > .05$ for all comparisons.

E) Immunoblot analysis to confirm the knockdown of indicated proteins compared to control hairpins. Actin is used as a loading control. Related to Figure 2.

Figure S3.

A) ELISA analysis to determine the levels of total SAPK/JNK (top) and phosphorylated SAPK/JNK (bottom) in cells left untreated, treated with PMA, or infected with *C. trachomatis* for the indicated times. Bars represent standard deviation from triplicate samples from one of two independent experiments.

B) Quantitative RT-PCR analysis reveals transcriptional activation of AP-1 target genes between 20 and 30 hours following *C. trachomatis* infection. Cells were infected with *C. trachomatis* or mock-infected for 20 or 30 hours. Total RNA was isolated and used for RT-PCR analysis. Expression analysis was normalized to host Beta-Actin as a control.

Depicted is the relative fold change (Infected/Uninfected) in the expression of the indicated genes at twenty and thirty hours post-infection (n=3). Shown is representative data from one of two independent experiments.

C) Natural language processing of top hits from the loss-of-function screen point towards a role for AP-1 signaling. Chilibot analysis was used in a candidate gene approach to examine interactions of loss-of-function hits and host signaling pathways. Shown are interactions of 4 hits that all interact with c-Jun based on literature analysis. Green arrows mean all sources show positive regulation while yellow means there are differing reports.

D) Schematic of JNK signaling cascade and targets of chemical inhibition. The JNK signaling cascade is activated under conditions such as stress, cytokine stimulation and growth factor binding. Activation of the JNK cascade begins with the phosphorylation of an upstream MAPKKK (such as MEKK1,4), which in turn phosphorylates a JNK associated MAPKK (MKK4/7) ultimately leading to the activation of the terminal MAPK (SAPK/JNK). The phosphorylation of SAPK/JNK leads to the activation of the AP-1 complex (depicted by JUN). Once JUN is phosphorylated, Pin1 must isomerize the phosphorylation directly on JUN in order for stable AP-1 transcription to occur. The isomerization of JUN phosphorylation leads to the expression of AP-1 dependent genes that include growth and differentiation factors, and genes associated with inflammation. The inhibitors used in this study block two distinct steps of this activation pathway. SP600125 blocks the phosphorylation of the terminal MAPK, SAPK/JNK, which prevents any phosphorylation of JUN. Juglone prevents the isomerization activity by Pin1, which leads to dampened AP-1 activity due to unstable phosphorylation of JUN. Related to Figure 3

Figure S4.

A) Chemical inhibition with SP600125 or Juglone inhibits the phosphorylation of c-Jun during infection with *C. trachomatis*. HeLa cells were infected with Chlamydia, and 10 hours post-infection cells were treated with the indicated inhibitor or vehicle control. For the washout cells were washed 20 hours post-infection to remove the inhibitor. Cells were then lysed 35 hours post-infection and analyzed for total p-c-Jun in cells. Loading was normalized to tubulin. Shown is a representative immunoblot from one of three independent experiments.

B) Chemical inhibition with SP600125 or Juglone does not alter activation of ERK or p38 and other signaling pathways. HeLa cells were infected with *C. trachomatis* and treated with vehicle alone, SP600125, or Juglone 20 hours post-infection. Thirty hours after infection cells were lysed and applied to PathScan Intracellular signaling arrays in duplicate per condition. Arrays were read and analyzed using the Odyssey infrared imaging system. The relative intensity of each spot was calculated using Odyssey software. Shown are the mean fluorescent intensities for each phosphorylated MAPK pathway for all inhibitor conditions +/- the standard deviation.

C) Combining both inhibitors at low concentrations increases growth inhibition. Cells were infected with Chlamydia and treated with the indicated vehicle alone or inhibitor 10 hours post-infection. 40 hours post-infection cells were lysed and titered onto fresh HeLa cells. 24 hours following re-infection cells were fixed and stained for *C. trachomatis* and the number of inclusions following each treatment was enumerated. Shown is the mean IFU produced from each condition from one independent experiment of three (n=4). p<.05 for treatment with both inhibitors by one-way ANOVA.

D) AP-1 transcription is needed for *C. trachomatis* growth. Cells were infected Cells were infected with Chlamydia and treated with the indicated vehicle alone or inhibitor 10 hours post-infection. Only for Tanshione IIa were multiple concentrations used. 40 hours

post-infection cells were lysed and titered onto fresh HeLa cells. 24 hours following reinfection cells were fixed and stained for *C. trachomatis* and the number of inclusions following each treatment was enumerated. (Left) Shown is the mean pg *C. trachomatis* 16s DNA per condition (n=4). No comparison is significant. (Right) Shown is the mean IFU produced from one independent experiment of three. All conditions $p < .05$ compared to DMSO control by one-way ANOVA. Related to Figure 4.

Supporting Tables

Table S1. GPS validation summary, Screen data, and Probe info

Worksheet1 - GPS screen Validation summary: Overview of the 175 candidate genes examined in the GPS screen validation. For each gene tested in each validation experiment (GPS clonal cell lines, Tagged Immunoblot, or Endogenous Immunoblot) it is indicated whether the results validated the original screen data produced.

Worksheet 2 – Merged GPS data for each probe to positive hits in GPS screen: For each hit that passed visual inspection and the deltaPSI threshold we show the average data for each probe for that ORF.

Worksheet 3 – Raw GPS Screen Data: For each individual probe that passed initial quality control both the calculated protein stability index from uninfected and infected conditions is shown. The intensity of each probe for each ORF is also listed for all bins.

Worksheet 4 – Sequence information for each probe present in the library/microarrays.

Table S2. Bioinformatics analysis summary.

Worksheet 1 – DAVID analysis was used as described in the methods. This worksheet summarizes the top 12 annotation clusters that were enriched among stabilized proteins

in the GPS screen.

Worksheet 2 – List of genes enriched in each annotation cluster from stabilized proteins

Worksheet 3 - DAVID analysis was used as described in the methods. This worksheet summarizes the top 12 annotation clusters that were enriched among destabilized proteins in the GPS screen.

Worksheet 4 - List of genes enriched in each annotation cluster from destabilized proteins

Table S3. Log2 Ratios for growth in Loss-of-Function screen (Experimentals and Controls)

Worksheet 1 – siRNA screen full data (experimentals): The experimental genes disrupted by siRNA are listed, along with fold change in *C. trachomatis* IFU production for each replicate, the mean fold change, and then number of individual duplexes that scored as positive hits in the pool deconvolution screen.

Worksheet 2 – siRNA Controls: The Mean fold change in *C. trachomatis* growth in control genes disrupted by siRNA.

Table S4. Customized Macro for plotting GPS histograms

A Macro used to rapidly graph probe distributions across all bins for both uninfected and infected conditions (Examples shown in Figure S1).

Supporting Online Material

Materials and Methods

Tissue Culture, Reagents, and General Procedures

HeLa, and 293T cells were maintained in Dulbecco's Minimum Essential Media supplemented with Penicillin/Streptomycin and 10% fetal bovine serum (Invitrogen). 293T and HeLa cells were transfected using the TransIT transfection reagent (Mirus). Lentiviruses were packaged in 293T cells transfected with the plasmid of interest as well as plasmids expressing VSVg and Gag-Pol-Rev (Luo et al., 2009). Viral infections were supplemented with hexadimethrine bromide at a concentration of 8 µg/ml. Transfection of siRNA oligonucleotides was performed with Dharmafect (Dharmacon) lipid transfection reagent according to the manufacturer's protocols. siRNA were purchased from Dharmacon as smart pools. A complete list of immunological reagents used in this study is below. Flow cytometry was performed on a BD-LSRII Flow Cytometer or a BD-FACS Calibur (Becton Dickinson). Data were collected using BD FACS Diva software (Becton Dickinson) and analysis was performed using FloJo software.

GPS validation was performed by first individually picking ORFeome clones from the arrayed entry library. Entry vectors were then cloned into the GPS vector using gateway recombination as described previously. All inserts were sequenced using the primer: 5'-AGCTGTACAAGTCCGAACTCGT-3'. The vectors were used to package virus and used to generate cell lines expressing individual GPS-ORFs.

EBs of *C. trachomatis* serovar L2 434/Bu were propagated within McCoy cell monolayers. A combination of glass bead disruption and sonication was used to

release EBs from infected McCoy cells. EBs were further purified by ultracentrifugation over Renograffin gradients, as previously described (15). Aliquots of *C. trachomatis* EBs were stored at -80° C in SPG buffer (250 mM sucrose, 10 mM sodium phosphate, and 5 mM L-glutamic acid, pH 7.2). Prior to infection with *C. trachomatis*, cells were cultured for 12-24 h in their respective media minus antibiotics. Cells were infected with *C. trachomatis* by adding media containing dilute EBs to host cells. Centrifugation was not used unless specified in the text. The multiplicity of infection (MOI) used for *C. trachomatis* was 3:1 unless indicated. DMEM alone was used for mock-infected cells.

Immunoblot analysis. For immunoblot analysis, cells were lysed at indicated timepoints following infection in Urea lysis buffer unless otherwise indicated (8M Urea, 150 mM NaCl, 0.1% NP-40) in the presence of a complete protease inhibitor cocktail (Roche Applied Science, Indianapolis, IN) and phosphatase inhibitor (Cell Signaling). Lysates were normalized for total protein content by measuring absorption at 280 nm or using a BCA test (Pierce). Normalized samples were subjected to SDS-PAGE analysis (BD and Lonza), transferred to nitrocellulose or PVDF (Licor), and immunoblotted with the following antibodies:

Actin (Licor), BNIP3L (AbCam), Ciao1 (AbCam), Dusp16 (AbCam), JNK (Cell signaling), p-JNK (Cell signaling), Jun (Cell signaling), p-JUN (Cell Signaling) Men1 (AbCam), Ncap-G (Santa Cruz), Pin1 (Cell Signaling), PTEN (AbCam), SNCG (AbCam), Stk24 (AbCam), Tubulin (Licor), USH1C (AbCam)

Automated image analysis. Infected cells were fixed and permeabilized with MeOH and stained for *Chlamydia* MOMP (FITC-MOMP, BioRad) for 1 hour. Stained cells were imaged with a Cellomics ArrayScan VTI automated microscope. Six fields per well of a

96-well plate were imaged at 20x magnification. First, cells were identified by their nuclei staining in channel 1 of Cellomics. Cells that scored positive in channel 1 were analyzed for Alexa-488 (inclusions) in channel 2. A minimum average intensity in the Alexa-488 channel was calculated by manual inspection and applied to each selected object. The selected objects that were above this threshold were shown in blue while those that were below are shown in orange. Once the threshold was determined, all of the plates were subjected to data analysis using vHCS Scan Target Activation software v5.1.2. Data were obtained by using vHCS View software and the number of inclusions in the well was identified as “valid object count” (VOC).

Immunofluorescence analysis. Cells were seeded on coverslips in 24 well dishes. The next day cells were infected with *C. trachomatis* at an MOI of 3. 24 hours following infection cells were fixed using paraformaldehyde and permeabilized using .1% tween in PBS. We then stained cells with anti-*Chlamydia* antibody linked to FITC and DAPI. Cells were analyzed at 20x using a NIKON Eclipse 200. At least 10-20 images were captured per coverslip. We then analyzed the average diameter of inclusions using imageJ analysis.

Quantitative PCR. To assess the levels of *C. trachomatis* present, we used a previously described qPCR method (Coers et al., 2011). Briefly, we isolated nucleic acid from infected cells using the DNeasy kit (Qiagen). *Chlamydia* 16S DNA was quantified by qPCR on an ABI Prism 7000 sequence detection system using primer pairs and dual-labeled probes. Using standard curves from known amounts of *Chlamydia* the levels of 16s DNA per well was calculated. For *in vivo* experiments the upper genital tract was isolated and DNA was isolated and the levels of *C. trachomatis* were determined relative to levels of host DNA as described previously (Gondek et al., 2012).

IFU Analysis

To assess the production of infectious progeny we used a standard IFU assay. Cells infected with *C. trachomatis* were lysed in H₂O with .1% NP-40. Cell lysates were then diluted in fresh media and these dilutions were titered onto 10⁴ HeLa cells. Twenty four hours following re-infection cells were fixed in ice cold MeOH and permeabilized in PBS containing .1% Tween. Chlamydia inclusions were then stained using FITC conjugated anti-MOMP antibody and host nuclei were stained using 1ug/ml DAPI. Total inclusions per well were counted and the number of infectious *C. trachomatis* produced was calculated.

AP-1 complex activation

For examination of AP-1 dependent transcription an AP-1 driven EGFP reporter cell line was created using pre-made Lentivirus (SAbioscience). After puromycin selection cells were infected with *C. trachomatis* for 30 hours or treated 10ng/ml of PMA for 10 hours and examined by flow cytometry using a FACs Calibur (BD) for EGFP induction. Plots were analyzed using FlowJo software.

JNK and p-JNK Activation

Cell lysates from cells infected for the indicated times were used as samples in a sandwich ELISA to detect levels of total JNK and p-JNK following infection (Cell Signaling). The manufacturer instructions were followed. Samples were tested for their absorbance 450 nm.

Chemical Inhibitors

The JNK inhibitor (SP600125) and Pin1 inhibitor (Juglone) were purchased from EMD Millipore for pathway analysis and used at the indicated concentrations. Tanshione IIa

was purchased from (Santa Cruz). For *in vitro* experiments Juglone was resuspended in EtOH, for *in vivo* experiments Juglone was resuspended in DMSO. SP600125 and Tanshione Ila were dissolved in DMSO for all experiments. Vehicle controls contain the appropriate solvent for each experiment.

Phospho-Array

Cells infected with *C. trachomatis* at an MOI of 3 for 20 hours were treated with DMSO alone, 1 μ M SP600125, or 1 μ M Juglone for 10 hours. Cells were processed and the arrays were conducted according to manufacturers directions for the Pathscan Intracellular Signaling Array Kit (Cell Signaling). Arrays were scanned and quantified using an Odyssey Infrared Imaging system and software (LiCor).

siRNA Screen. siRNA smart pools were cherry picked into 96 well plates from the complete Dharmacon siRNA genome set at the Harvard Institute of Chemistry and Cell Biology (ICCB). The outer wells of each plates were excluded. Each plate contained 6 non-targeting controls and 6 positive controls used to optimize the assay. HeLa cells were seeded at a density of 2.5×10^3 into 96-well plates. Each siRNA was transfected in triplicate for 72 hours. Cell viability was examined at 72 hours and scored on 0-5 scale (0=all cells dead 5=no obvious cell death). Cells that scored 2 or less were not analyzed further. Cells were then infected with 10^4 IFU of *C. trachomatis* for 48 hours. Cells were then lysed in H₂O with .1% NP-40, diluted 1:1000 in fresh media and re-seeded into 96 well plates containing 10^4 normal HeLa cells. Twenty-four hours following infection, cells were fixed with ice-cold MeOH for 30 minutes. Cells were washed two times with PBS containing 0.1% tween. Cells were then stained using DAPI and an antibody to *C. trachomatis* MOMP (Bio-Rad). Cells were quantified by automated microscopy as described above. The mean number of IFU produced by non-targeting controls for each

plate was calculated. A fold-change in *C. trachomatis* growth was calculated against non-targeting mean for each plate. A mean fold-change was then calculated for all triplicate samples. Cells that inhibited growth more than 2-fold were picked for a deconvolution screen which was run identically to the primary screen described above.

Stable knockdown cells were created using standard lentiviral transduction described above. shRNA (2 per gene) vectors were purchased from the TRC library. Lentiviral particles were packaged according to manufacturer's instructions. Following lentiviral production and transduction cells were selected using 1 μ g/ml Puromycin. Knockdown of experimental proteins was confirmed by immunoblot analysis.

GPS Screen. The GPS screen was conducted essentially as described (Yen et al., 2008). Cells were mock-infected or infected with *C. trachomatis* for 24 hours. Infection was confirmed visually by the presence of inclusions in almost all cells. The general workflow of the GPS screen is as follows. 293T cell libraries were sorted into either 7 bins, based on their EGFP/DsRed ratio. Approximately equal numbers of cells were sorted into each bin, with the outermost bins receiving slightly fewer cells than those in the middle. We sorted a minimum of 1.2 million cells per bin. Sorting was carried out at the Immune Diseases Institute at Harvard Medical School with the assistance of Natasha Barteneva. Following sorting, cells were pelleted and frozen at -80°C . Pellets were subsequently thawed and lysed in 10 mM Tris pH 8.0, 10 mM EDTA, 0.5% SDS, and 0.2 mg/ml Proteinase K at 55°C overnight with agitation. Genomic DNA (gDNA) was extracted using Phaselock tubes with phenol:chloroform and then chloroform. RNase A was added to a final concentration of 25 $\mu\text{g}/\text{ml}$ and following incubation overnight at 37°C , gDNA was extracted using Phaselock tubes, as above. DNA was ethanol precipitated (with glycogen), recovered by centrifugation, and washed three times with 75% ethanol. The dried, resuspended pellet was PCR amplified with Takara hot start

polymerase (Takara RR006B) using common PCR primers as described (Yen and Elledge, 2008). PCR amplified DNA was transcribed with T7 using Ambion MEGAscript and purified with Qiagen RNeasy kits. RNA was labeled with a ULS labeling kit (Kreatech: unsorted samples-Cy5, sorted samples-Cy3). Hybridization was performed on custom Agilent DNA microarrays printed as 4 x 44k arrays according to manufacturer's protocols. The probe sequences used are listed in the supplemental table. Microarrays were read using an Agilent scanner. The GPS screen was performed using version 3.1 of the ORFeome collection. PSI was calculated as described (Yen et al., 2008). Percent shift was calculated by summing absolute values of the subtracted relative abundance from probes across all bins.

GPS Data Analysis. Probes were first filtered by removing probes with signals below five-time the average background signal. Probes with signals less than zero were reset to zero. Microarrays from each bin were normalized within each screen based on their spike-in control signals. After filtering low signal probes and normalizing, we examined the EGFP signals for all probes within a single bin between treated and untreated conditions for every bin to confirm probe and hybridization reliability. We next calculated the PSI for each probe and compared those between treated and untreated conditions. These numbers are reported in the supplementary table. The average PSI of all probes, for each condition, was determined and normalization was performed as necessary. A Δ PSI was calculated by subtracting the PSI numbers of the uninfected from those of the infected. We rank ordered probes based on Δ PSI and used a custom macro in Microsoft Excel to graph the distribution for every probe across bins, comparing infected and uninfected conditions on each graph, for every probe that passed our low signal cut-off (Table S4). We have included a blank excel file with the coding for this macro as supplementary table 5. Visual inspection of the graphs was essential for high validation

rates and to easily discriminate against hits that are influenced by noise seen in microarray studies. Graphs were ranked based on the Δ PSI and were visually inspected one at a time to determine if there was a significant probe shift. We have listed those ORFs that had a sufficient Δ PSI and passed visual inspection. We often found that a high Δ PSI could be attributed to erroneous noise in outside bins, making visual inspection essential. Genes that showed a significant shift from multiple probes (when available) were designated for further study and are listed in Table S1 worksheet 2.

Bioinformatic Analysis

We used DAVID bioinformatics resources to identify enriched annotation clusters within the GPS dataset as done previously (Huang da et al., 2009). We uploaded our stabilized and destabilized protein lists independently into DAVID and used the human proteome as the background list. We used cluster analysis to identify redundant enriched terms for each group through several categories including KEGG pathway and Gene Ontology terms. We listed the top enriched clusters including enrichment scores and genes identified in Table S2.

We also used natural language processing analysis in a candidate gene approach to identify connections in the published literature among genes found in the loss-of-function screen as done by others previously (Chittenden et al., 2008). We used Chilibot freeware and searched for interactions between c-Jun and each of the 14 loss-of-function hits. The resulting findings were used to create a graphic representation of these interactions in Chilibot software (Chen and Sharp, 2004).

Mice and *in vivo* inhibitor treatment

C57BL/6 were purchased from The Jackson Laboratory and were maintained and cared for within the Harvard Medical School Center for Animal Resources and Comparative

Medicine (Boston, MA). All mice were treated with 2.5mg of medroxyprogesterone subcutaneously seven days prior to infection in order to normalize the murine estrous cycle. Mice were infected transcervically with 10^6 IFU of *C. trachomatis*. For inhibitor treatments mice were injected IP and transcervically with vehicle alone, 10 mg/kg of SP600125 per injection route (Wang et al., 2004), and 1 mg/kg of Juglone per injection route (Kim et al., 2010) similar to previous studies. All experiments were approved by Institutional Animal Care and Use Committee. In all experiments ten mice per group were used.

Supplementary ReferencesChen, H., and Sharp, B.M. (2004). Content-rich biological network constructed by mining PubMed abstracts. *BMC bioinformatics* 5, 147.

Chittenden, T.W., Howe, E.A., Culhane, A.C., Sultana, R., Taylor, J.M., Holmes, C., and Quackenbush, J. (2008). Functional classification analysis of somatically mutated genes in human breast and colorectal cancers. *Genomics* 91, 508-511.

Coers, J., Gondek, D.C., Olive, A.J., Rohlfing, A., Taylor, G.A., and Starnbach, M.N. (2011). Compensatory T cell responses in IRG-deficient mice prevent sustained *Chlamydia trachomatis* infections. *PLoS pathogens* 7, e1001346.

Gondek, D.C., Olive, A.J., Stary, G., and Starnbach, M.N. (2012). CD4+ T cells are necessary and sufficient to confer protection against *Chlamydia trachomatis* infection in the murine upper genital tract. *J Immunol* 189, 2441-2449.

Huang da, W., Sherman, B.T., and Lempicki, R.A. (2009). Systematic and integrative analysis of large gene lists using DAVID bioinformatics resources. *Nature protocols* 4, 44-57.

Kim, S.E., Lee, M.Y., Lim, S.C., Hien, T.T., Kim, J.W., Ahn, S.G., Yoon, J.H., Kim, S.K., Choi, H.S., and Kang, K.W. (2010). Role of Pin1 in neointima formation: down-regulation of Nrf2-dependent heme oxygenase-1 expression by Pin1. *Free radical biology & medicine* 48, 1644-1653.

Wang, W., Shi, L., Xie, Y., Ma, C., Li, W., Su, X., Huang, S., Chen, R., Zhu, Z., Mao, Z., *et al.* (2004). SP600125, a new JNK inhibitor, protects dopaminergic neurons in the MPTP model of Parkinson's disease. *Neuroscience research* 48, 195-202.